

# Production and detection of atomic hexadecapole at Earth's magnetic field

V. M. Acosta,<sup>1</sup> M. Auzinsh,<sup>2</sup> W. Gawlik,<sup>3</sup> P. Grisins,<sup>2</sup> J. M. Higbie,<sup>1</sup> D. F. Jackson Kimball,<sup>4</sup> L. Krzemien,<sup>3</sup> M. P. Ledbetter,<sup>1</sup> S. Pustelny,<sup>3</sup> S. M. Rochester,<sup>1</sup> V. V. Yashchuk,<sup>5</sup> and D. Budker<sup>1,6,\*</sup>

<sup>1</sup>Department of Physics, University of California, Berkeley, CA 94720-7300

<sup>2</sup>Department of Physics, University of Latvia, 19 Rainis blvd, Riga, LV-1586, Latvia

<sup>3</sup>Center for Magneto-Optical Research, Institute of Physics, Jagiellonian University, Reymonta 4, 30-059 Kraków, Poland

<sup>4</sup>Department of Physics, California State University – East Bay, 25800 Carlos Bee Blvd., Hayward, CA 94542, USA

<sup>5</sup>Advanced Light Source Division, Lawrence Berkeley National Laboratory, Berkeley CA 94720, USA

<sup>6</sup>Nuclear Science Division, Lawrence Berkeley National Laboratory, Berkeley CA 94720, USA

PACS numbers:

Anisotropy of atomic states is characterized by population differences and coherences between Zeeman sublevels. It can be efficiently created and probed via resonant interactions with light, the technique which is at the heart of modern atomic clocks [1] and magnetometers [2]. Polarization moments (PM) characterizing anisotropy of a state with total angular momentum  $F$  are coefficients in the expansion of the density matrix into irreducible tensor operators of rank  $\kappa = 0, \dots, 2F$  and projection  $q = -\kappa, \dots, \kappa$ . The lowest PMs are population ( $\kappa = 0$ ), orientation ( $\kappa = 1$ ), and alignment ( $\kappa = 2$ ). Recently, non-linear magneto-optical techniques have been developed for selective production and detection of higher PMs, hexadecapole ( $\kappa = 4$ ) and hexacontatetrapole ( $\kappa = 6$ ), in the ground states of the alkali atoms [3, 4]. Extension of these techniques into the range of geomagnetic fields is important for practical applications. This is because hexadecapole polarization corresponding to the  $\Delta M = 4$  Zeeman coherence, with maximum possible  $\Delta M$  for electronic angular momentum  $J = 1/2$  and nuclear spin  $I = 3/2$ , is insensitive to the nonlinear Zeeman effect (NLZ). This is of particular interest because NLZ normally leads to resonance splitting and systematic errors in atomic magnetometers. However, optical signals due to the hexadecapole moment decline sharply as a function of magnetic field. In this Letter, we report a novel method that allows selective creation of a macroscopic long-lived ground-state hexadecapole polarization. The immunity of the hexadecapole signal to NLZ is demonstrated with  $F = 2$   $^{87}\text{Rb}$  atoms at Earth's field.

Figure 1 shows a schematic of the experimental apparatus. A diode laser tuned to the D1 line interacts with  $^{87}\text{Rb}$  atoms contained in an antirelaxation coated cell, to which a magnetic field is applied. The  $F = 2$  ground-

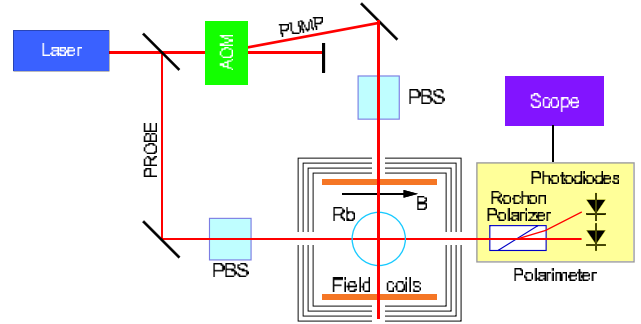


FIG. 1: Schematic of the experimental apparatus. The modulated pump light beam is used to polarize  $^{87}\text{Rb}$  atoms. The unmodulated probe beam is used to detect the evolution of the atomic polarization moments via induced optical rotation. AOM: acousto-optic modulator; PBS: polarizing beam splitters. See Methods.

state atoms are pumped using a sequence of short pulses of linearly polarized light with a repetition rate determined by the Larmor precession frequency of the atomic angular momentum. At the end of the sequence, the pump light is blocked. The evolution of the atomic polarization is observed by measuring the angle of optical rotation of an unmodulated probe beam whose initial polarization is the same as that of the pump. An alternative arrangement where the pump beam itself was attenuated after the pumping cycle and used for probing (without modulation) was also used in some of the experiments.

The symmetry properties of polarization moments can be illustrated using angular-momentum probability surfaces [5, 6, 7], in which the distance between the origin and the surface in a given direction is proportional to the probability of finding maximal projection  $m = F$  in that direction. Figure 2 shows such surfaces for the quadrupole ( $\kappa = 2$ ) and hexadecapole ( $\kappa = 4$ ) moments. The surfaces shown correspond to combinations of  $q = -2$  and  $2$  for the quadrupole, and  $q = -4$  and  $4$  for the hexadecapole with the quantization axis along the magnetic field [15]. The atomic angular momentum precesses at the Larmor frequency  $\Omega_L$  proportional

\*Electronic address: budker@berkeley.edu

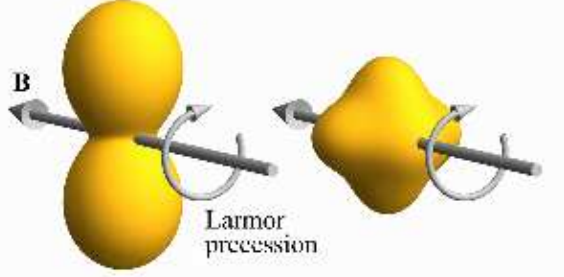


FIG. 2: Angular momentum probability surfaces for quadrupole (left) and hexadecapole (right) for  $F = 2$ . The shown polarizations are transverse to the quantization axis, which is chosen along the magnetic field. The anisotropies and polarization surfaces undergo Larmor precession around the magnetic field.

to the applied magnetic field. Consider the “peanut”-shaped quadrupole moment. When the peanut has rotated by an angle  $\pi$ , it is impossible to differentiate it from its initial state, i.e., it has a 2-fold symmetry. Consequently, efficient pumping of the quadrupole is achieved with light modulated at an angular frequency  $2\Omega_L$ . Precession of the quadrupole results in optical rotation of the probe light oscillating at  $2\Omega_L$ . In general, a PM with a component  $q$  has  $|q|$ -fold symmetry and can therefore be pumped with light harmonically modulated at  $|q|\Omega_L$  or with short pulses at a repetition rate of  $|q|\Omega_L/(2\pi n)$ , where  $n$  is an integer. The polarization moments prepared in this way produce an optical rotation signal at  $|q|\Omega_L$  [3, 4]. Polarization moments with  $|q|$ -fold symmetry can be detected by demodulating the optical rotation signal at  $|q|\Omega_L$ .

By pumping at  $4\Omega_L$ , hexadecapole can be created without the presence of the quadrupole [3, 4]. This is desirable, as the presence of the typically much larger quadrupole signal makes it difficult to observe the hexadecapole. Unfortunately, the amount of hexadecapole pumped in this way rapidly decreases with the magnetic field strength, as seen in Figure 3 (bottom trace). This can be understood by recalling that a photon is a spin-one particle, so it is described by tensor operators of rank  $\kappa \leq 2$ . Consequently, two photons are needed to produce an atomic state of  $\kappa = 4$  (hexadecapole). When pumping at  $4\Omega_L$ , both photons must interact with the atoms in a single pulse in order to create hexadecapole. The alternative mode of hexadecapole creation, two single-photon processes occurring during separate cycles, is ineffective when pumping in this manner, as it would require the survival of quadrupole between the pumping pulses. In fact, each successive pumping cycle creates a quadrupole that is orthogonal to the quadrupole that was created in the previous cycle. This is because the latter has rotated by  $\pi/2$  due to Larmor precession over the duration of the cycle. Thus, the quadrupole polarizations

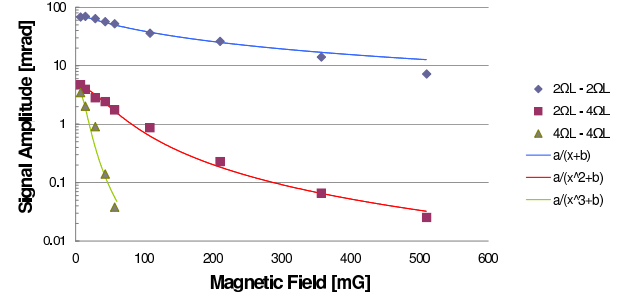


FIG. 3: Magnetic-field dependence of optical rotation amplitudes for quadrupole (blue diamonds), hexadecapole pumped with light modulated at  $2\Omega_L$  (maroon squares), and hexadecapole pumped at  $4\Omega_L$  (green triangles). The quadrupole and hexadecapole, pumped at  $2\Omega_L$  decrease much more slowly with magnetic field compared to hexadecapole pumped at  $4\Omega_L$ . The solid lines are fits by ad-hoc functions.

from successive cycles cancel the transverse quadrupole (and the net result is a longitudinal quadrupole, seen as a “doughnut” in the inset of Fig. 4, which does not aid in creation of transverse hexadecapole). As the field increases, the pumping period  $[T = 2\pi/(4\Omega_L)]$  decreases, reducing the probability of a process occurring which involves interactions with two photons in a single pulse. Even using the strongest pump power available in the experiment (4 mW), the hexadecapole signals cannot be distinguished above noise at the Earth’s field ( $4\Omega_L/2\pi \approx 1.4$  MHz) in this scheme.

An alternative method for efficiently pumping hexadecapole is to use light modulated at  $2\Omega_L$ , producing both quadrupole and hexadecapole. In this scheme, the requirement of pumping the hexadecapole in a single pulse is alleviated as the hexadecapole can be obtained by “promoting” the quadrupole polarization with just a single-photon interaction. This method allows one to obtain hexadecapole signals that, while they still decrease with magnetic field in the present experiment, nevertheless remain observable at the Earth field (Fig. 3). The remaining decrease in the hexadecapole signal is related to nonlinearity of the interaction, in this case, at the probing stage. The decrease is qualitatively reproduced by a model density-matrix calculation to be described elsewhere. Note that because we use an antirelaxation-coated cell, atoms pumped into a state with quadrupole polarization may leave the light beam and bounce around the cell for a relatively long time (on the order of the polarization-relaxation time), before they interact with the light again and are pumped into a state with hexadecapole polarization. Note also that the decrease of the quadrupole signal with magnetic field seen in Fig. 3 is a consequence of nonlinearity in the probing process at the relatively high powers required for probing hexadecapole (and which we use for quadrupole to be able to compare the two signals directly). With the single-beam arrangement, we verified that the quadrupole signal did not drop

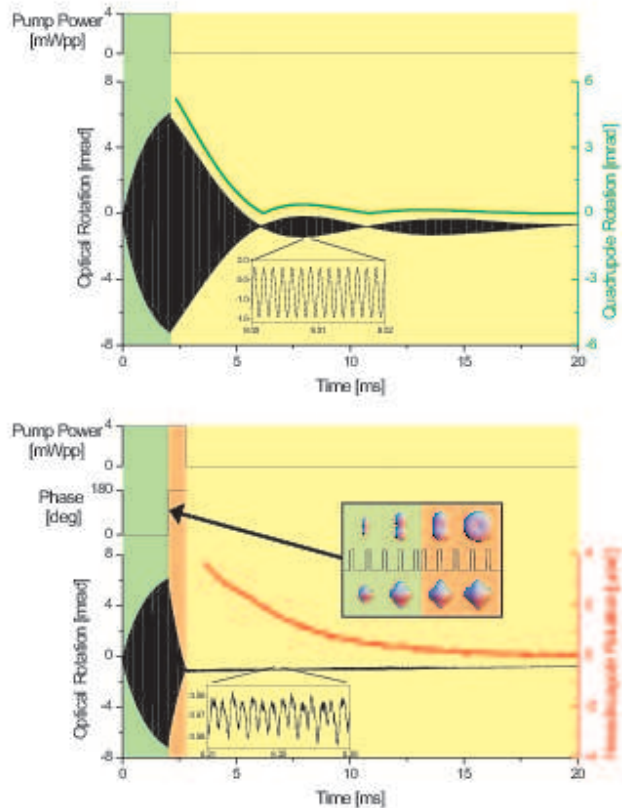


FIG. 4: Comparison of the demodulated quadrupole signal (top) without phase flip (see text) and of the hexadecapole signal obtained with phase flip (bottom). For the case of pumping without phase flip (top), the signal demodulated at  $2\Omega_L$  is plotted alongside the raw optical rotation signal. The inset on the top plot is a blowup of the raw optical-rotation signal during a revival stage of the quadrupole-signal beats occurring due to the nonlinear Zeeman effect (NLZ). This signal on the bottom plot (with phase flip) is demodulated at  $4\Omega_L$ , and the resulting curve shows the absence of the beats related to NLZ. The inset on the right shows the details of the pumping pulses near the phase flip, along with the angular-momentum probability surfaces characterizing the ensemble at different stages of pumping. The magnetic field around which these surfaces precess is normal to the page.

for magnetic fields up to 268 mG with a low probe-light power of  $3 \mu\text{W}$ .

Figure 4 (top) shows the optical rotation signal obtained with 1500 square pump pulses with repetition rate of  $2\Omega_L/(2\pi) \approx 714 \text{ kHz}$  and a duration of  $1/8$  of a period. Significant beating of the signal is observed after the pulse sequence ends, which is due to NLZ (the effect of NLZ on nonlinear magneto-optical rotation is discussed in Ref. [8]). Fits of the demodulated quadrupole signal indicate the presence of three close frequencies in the time dependence of the optical rotation with a splitting between adjacent frequencies of  $\approx 72 \text{ Hz}$  close to the value of the NLZ splitting,  $\delta_{NLZ} = 74.65 \text{ Hz}$  for this field.

The overall exponential decay time ( $\tau \approx 4.7 \text{ ms}$ ) is determined by the relaxation of the PMs due to dephasing from collisions and magnetic-field inhomogeneities, and by residual probe-power broadening. Buried under the much larger quadrupole signal there is also hexadecapole signal producing modulation of the optical rotation at  $4\Omega_L$ . Unfortunately, due to intrinsic nonlinearities in the detection electronics as well as those due to the interaction of atoms with a strong probe light [9], the large quadrupole signal leads to the presence of a “false hexadecapole” signal at  $4\Omega_L$ , and it is hard to distinguish the two contributions.

The solution implemented in the present work is to eliminate the quadrupole just before probing. To accomplish this, the pumping is separated into two stages. The first stage is the same as in the pumping scheme above: the atoms are pumped at  $2\Omega_L$  for  $\approx 1500$  cycles. Then, the phase of the pumping is flipped by  $\pi$  (see inset in the bottom plot of Fig. 4). The quadrupole is now pumped orthogonally to its previous alignment and the resulting sum of orthogonal quadrupole moments leaves no net transverse alignment (the resulting doughnut shape, corresponding to longitudinal alignment that causes no optical rotation of the probe light, is shown inset at the bottom plot in Fig. 4). However, the hexadecapole produced before and after the phase flip is identical, so it continues to be pumped even after the phase flip. After  $\approx 500$  cycles, the quadrupole reaches a minimum and the pump is shut off. Figure 4 (bottom) demonstrates the phase-flip pumping scheme and the resulting signal. The quadrupole signal (not shown) is reduced by about a factor of 40 in this scheme, allowing for the reliable recovery of the signal due to the hexadecapole moment. The demodulated hexadecapole signal is a simple exponential decay ( $\tau = 4.2 \text{ ms}$ ), clearly demonstrating the absence of NLZ-induced beating.

In an additional series of measurements, we studied the dependence of the quadrupole and hexadecapole optical-rotation signals on the gradient of the magnetic field. These measurements (Fig. 5) confirmed the expected (see, for example, Ref. [10]) four-times higher sensitivity of the hexadecapole to field gradients compared to the quadrupole.

In this work we have demonstrated a way to create and detect macroscopic hexadecapole polarization (corresponding to a  $\Delta M = 4$  Zeeman coherence) in the geomagnetic field range. The amount of hexadecapole created at these fields was dramatically enhanced by pumping at  $2\Omega_L$ , the frequency associated with efficient production of the (lower-rank) quadrupole moment. Phase flipping allowed the elimination of the large quadrupole signal in order to effectively uncover the smaller hexadecapole signal. The resulting hexadecapole signal demonstrates the absence of beating associated with the nonlinear Zeeman effect. The NLZ-free hexadecapole signals are attractive for applications in atomic magnetometry because the linear relation between the magnetic field and the spin-precession frequency is maintained over the

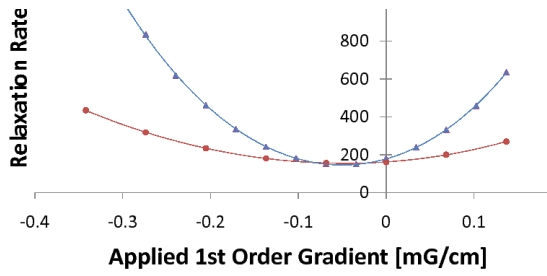


FIG. 5: The dependence of the observed relaxation rates for the quadrupole and hexadecapole signals on the magnetic-field gradient applied in the direction of the magnetic field. In both cases, pumping was with light pulsed at a repetition rate of  $2\Omega_L/(2\pi)$  at  $B \approx 108$  mG, and the relaxation was determined from the optical rotation after the pump light was shut off. Solid lines show fits to fourth-order polynomials; the ratio of curvatures near the vertex is consistent with the expected four times higher sensitivity of the hexadecapole to gradients [10].

geophysical field range. However, a shortcoming of the present method from the point of view of practical applications is the relative smallness of the hexadecapole signal. This is related to the necessity of employing a nonlinear interaction for probing hexadecapole polarization via optical rotation (similar to the case of pumping) [3]. In future work, it may be possible to overcome this by monitoring the hexadecapole moment via fluorescence detection [11, 12, 13].

## Acknowledgements

The authors acknowledge stimulating discussions with T. Karaulanov, and E. Corsini. This work has been supported by an ONR MURI program, NSF, and KBN grant # 1 P03B 102 30. S.P. is a scholar of the Foundation for Polish Science.

## Methods

A New Focus Vortex diode laser tuned to the  $^{87}\text{Rb}$   $F = 2 \rightarrow F' = 2$  transition on the D1 (795 nm) line was separated into two beams: a 4-mW linearly polarized pump beam modulated with an acousto-optic modulator (AOM, driven at 80 MHz) and a continuous probe beam with the same initial polarization. The probe power was  $25 \mu\text{W}$  for the data of Figs. 4 and 3 and  $9 \mu\text{W}$  for the data of Fig. 5. The laser frequency was fine-tuned to maximize the hexadecapole signal. Additional data were taken with a single laser beam serving as both pump and probe, tuned to the  $F = 2 \rightarrow F' = 1$  transition. The Rb atoms were housed in an evacuated glass cell with paraffin antirelaxation coating [14] contained in an oven maintaining the cell at  $42^\circ\text{C}$ . Four layers of  $\mu$ -metal shielding and a multi-order gradient-coil system were used to maintain a stable magnetic field of 510 mG. The angle of polarization of the outgoing probe beam was measured using a Rochon polarizing beam splitter and a high-speed, large area photodiode-op-amp circuit.

- 
- [1] Vanier, J. & Audoin, C. *The quantum physics of atomic frequency standards* (A. Hilger, Bristol ; Philadelphia, 1989).
  - [2] Budker, D. & Romalis, M. V. Optical magnetometry. *Nature Physics* **3**, 227–234 (2007).
  - [3] Yashchuk, V. V. *et al.* Selective addressing of high-rank atomic polarization moments. *Phys. Rev. Lett.* **90**, 253001 (2003).
  - [4] Pustelny, S. *et al.* Pump-probe nonlinear magneto-optical rotation with frequency-modulated light. *Phys. Rev. A* **73**, 023817 (2006).
  - [5] Auzinsh, M. Angular momenta dynamics in magnetic and electric field: classical and quantum approach. *Can. J. Phys.* **75**, 853–72 (1997).
  - [6] Rochester, S. M. & Budker, D. Atomic polarization visualized. *Am. J. Phys.* **69**, 450–4 (2001).
  - [7] Alexandrov, E. B. *et al.* Dynamic effects in nonlinear magneto-optics of atoms and molecules: review. *J. Opt. Soc. Am. B* **22**, 7–20 (2005).
  - [8] Acosta, V. *et al.* Nonlinear magneto-optical rotation with frequency-modulated light in the geophysical field range. *Phys. Rev. A* **73**, 053404 (2006).
  - [9] Series, G. W. Theory of the modulation of light in optical pumping experiments. *Proc. Phys. Soc.* **88**, 957–968 (1966).
  - [10] Pustelny, S., Jackson Kimball, D. F., Rochester, S. M., Yashchuk, V. V. & Budker, D. Influence of magnetic-field inhomogeneity on nonlinear magneto-optical resonances. *Phys. Rev. A* **74**, 063406 (2006).
  - [11] Okunevich, A. I. On the possibility of detecting the transverse component of the hexadecapole moment of atoms in fluorescent emission. *Opt. Spectrosc.* **91**, 177–83 (2001).
  - [12] Auzinsh, M. P., Tamanis, M. Y. & Ferber, R. S. Zeeman quantum beats after optical depopulation of the ground electronic state of diatomic molecules. *Sov. Phys. JETP* **63**, 688–693 (1986).
  - [13] Ducloy, M. Nonlinear effects in optical pumping of atoms by a high-intensity multimode gas laser. General theory. *Phys. Rev. A* **8**, 1844–59 (1973).
  - [14] Alexandrov, E. B. *et al.* Light-induced desorption of alkali-metal atoms from paraffin coating. *Phys. Rev. A* **66**, 042903/1–12 [Erratum: *Phys. Rev. A* **70**, 049902(E) (2004)] (2002).
  - [15] In terms of coherences between Zeeman sublevels, these anisotropies correspond to  $\Delta M = 2$  and  $\Delta M = 4$  coherences, respectively.